Analysis of Novel Approach to Design of Ultra-wide Stopband Microstrip Low-Pass Filter Using Modified U-Shaped Resonator

Gholamreza Karimi, Ali Lalbakhsh, Khatereh Dehghani, and Hesam Siahkamari

A novel microstrip low-pass filter is presented to achieve an ultra-wide stopband with 11 harmonic suppression and very sharp skirt characteristics. The filter is composed of a modified U-shaped resonator (which creates two fully adjustable transmission zeroes), a T-shaped resonator (which determines a cut-off frequency), and four radial stubs (which provide a wider stopband). The operating mechanism of the filter is investigated based on a proposed equivalent-circuit model, and the role of each section of the proposed filter in creating null points is theoretically discussed in detail. The presented filter with 3 dB cut-off frequency (f_c = 2.35 GHz) has been fabricated and measured. Results show that a relative stopband bandwidth of 164% (referred to as a 22 dB suppression) is obtained while achieving a high figure-of-merit of 15,221.

Keywords: Microstrip low-pass filter, U-shaped resonator, ultra-wide stopband.

Manuscript received Feb. 13, 2014; revised May 6, 2015; accepted May 20, 2015.

Gholamreza Karimi (corresponding author, ghkarimi@razi.ac.ir) is with the Department of Electrical Engineering, the Faculty of Engineering, Razi University, Kermanshah, Iran.

Ali Lalbakhsh (ali.lalbakhsh@yahoo.com) is with the Department of Engineering, Kermanshah Branch, Islamic Azad University, Kermanshah, Iran.

Khatereh Dehghani (khatere_dehghan@yahoo.com) is with the Department of Electrical Engineering, Kermanshah Branch, Islamic Azad University, Kermanshah, Iran.

Hesam Siahkamari (hesamsiahkamary@yahoo.com) is with the Department of Electrical Engineering, the Faculty of Engineering, Razi University, Kermanshah, Iran.

I. Introduction

A microstrip low-pass filter (LPF) with compact size and high performance is one of the most important components in microwave circuits. This component is characteristically low-cost and easy to fabricate, as well as being easy to combine with other microwave circuit components [1]. There are a lot of techniques to simultaneously achieve compact size and high performance in relation to microstrip LPFs. Employing planar resonators [2]–[6] is one such technique. Another such technique is to use modified stepped-impedance hairpin resonators [2]. Although the authors of [2]–[3] could achieve a filter with ultra-wide stopband by employing radial stubs and shunt open stubs at the feed points of a center-fed coupled-line hairpin resonator, it provided a gradual roll-off.

To construct a microstrip LPF of compact design that can achieve an ultra-wide stopband, loaded radial-shaped patches were used in [4]–[5]. However, the proposed microstrip LPFs of [4]–[5] introduced a low insertion loss in the stopband. Adding a pair of stepped-impedance open stubs loaded on both ends of a high-impedance microstrip line was a proposed solution by [6] to improve the stopband characteristic in this kind of structure. In a similar procedure, both triangular patch resonators and polygonal patch resonators were introduced in [7]; however, the roll-off was not sharp enough. The authors of [8] employed properly arranged rat-race directional couplers to operate as bandstop transversal filtering sections to extend a stopband. Although this approach is new, it increases the circuit size. In [9], a single T-shaped resonator in combination with a novel suppressing cell was utilized to realize an LPF with 5

harmonic suppression. In [10], a broadside-coupled microstrip-coplanar waveguide was utilized to design an LPF with extremely wide stopband. In spite of this extremely wide stopband, the filter failed to provide a sharp roll-off. The presented filter in [11], which employed a resonator with slotted ground plane, suffered from the same problem. In terms of investigating the operating mechanisms of microstrip filters, several theoretically-based approaches have been explained in some recently published papers [12]–[14].

In this paper, a novel approach to designing an LPF is presented. Unlike the majority of the literature related to the design of microstrip filters, here we focus on the theoretical aspects of resonator design; by doing so, the presented analysis can be generalized to other microwave components. For instance, by employing the presented modified U-shaped resonator and making an appropriate use of extracted equations, transmission zeroes can be adjusted to suppress harmonics in different microwave components such as power dividers or diplexers [15].

Firstly, in this paper, a modified harmonic-suppressing U-shaped resonator and its equivalent LC circuit are presented and analyzed. Secondly, a T-shaped resonator is adopted in the aforementioned resonator, and finally, bandstop filters in the form of radial stubs are implemented. Thus, an ultra-wide stopband, from 2.35 GHz up to 26 GHz, with an attenuation of more than 22 dB is achieved.

II. Design of Harmonic-Suppressing Resonator

1. Equivalent Circuit and LC Parameters Extraction

The geometric structure of the novel U-shaped resonator and its LC circuit are depicted in Fig. 1. Since the modified U-shaped resonator is both vertically and horizontally symmetrical, the proposed LC circuit is also symmetrical. In Fig. 1(b), L_1 and L_2 represent the inductance of the high impedance transmission line; L_3 is the resultant inductance of each open stub; C_1 is the sum of the capacitances of the junction discontinuities between the main feed line and two upper and lower high-impedance lines; C_2 is the series coupling capacitance between the two identical stubs; and C_3 is the sum of metal–insulator–metal capacitances and shunt capacitance associated with the gap ("S" in Fig. 1(a)). The resonator's dimensions in Fig. 1(a) are as follows: $l_1 = 2.05$, $l_2 = 1.69$, $l_3 = 5.4$, $l_4 = 2.6$, $l_5 = 8.24$, $w_1 = 0.13$, $w_2 = 0.3$, $w_3 = 2.0$, $w_4 = 2.23$, $w_5 = 0.4$, and $S = 0.89$ (all in millimeters). The values of the lumped elements (L_1, L_2, L_3, C_1, C_2, and C_3) can be extracted by use of the methods discussed in [1], and then they are optimized slightly to achieve a very similar response to electromagnetic (EM) simulation. The yielded values are

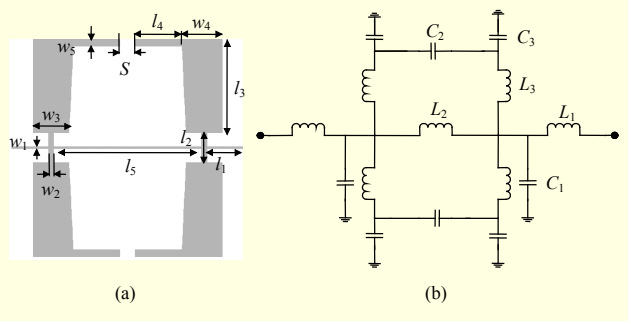

Fig. 1. (a) Layout of proposed U-shaped resonator and (b) LC equivalent circuit.

$L_1 = 0.61$ nH, $L_2 = 3.5$ nH, $L_3 = 0.6$ nH and $C_1 = 1.22$ pF, $C_2 = 0.003$ pF, $C_3 = 1.2$ pF. Figure 2(a) shows the EM and LC results.

2. Characteristics of Novel U-Shaped Resonator

The proposed modified U-shaped resonator introduces two adjustable transmission nulls at 5.5 GHz and 6.5 GHz. It is clear that C_1 and L_1 do not contribute to make these resonance frequencies, whereas C_2, C_3, L_2, and L_3 do; L_3 and C_3 create a deep transmission null at around 6 GHz, while the presence of the gap capacitor (C_2) turns this transmission zero into two separate zeroes with equal distance from 6 GHz. Figure 2(b) shows the positions at where multiple zeroes occur for three different values of C_2. As it is demonstrated in Fig. 2(b), for

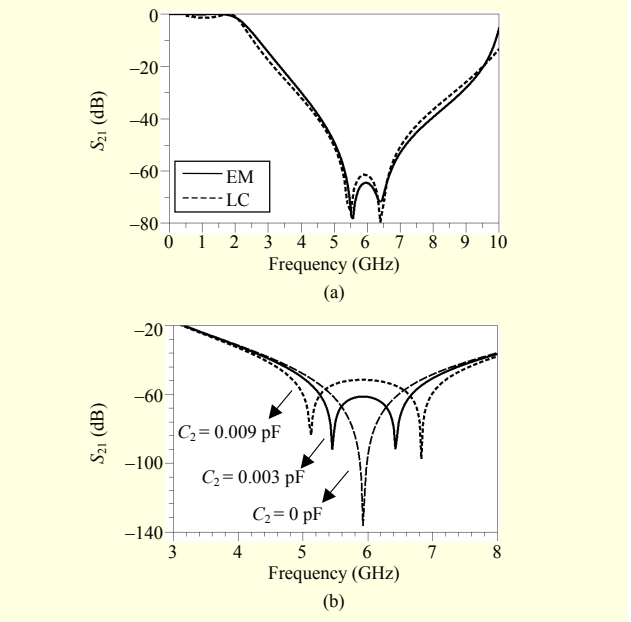

Fig. 2. (a) EM and circuit simulation results of proposed U-shaped resonator on substrate with relative dielectric constant of 3.38 and thickness of 0.508 mm and (b) effect of gap capacitance on location of multiple zeroes.

ETRI Journal, Volume 37, Number 5, October 2015
http://dx.doi.org/10.4218/etrij.15.0114.0188

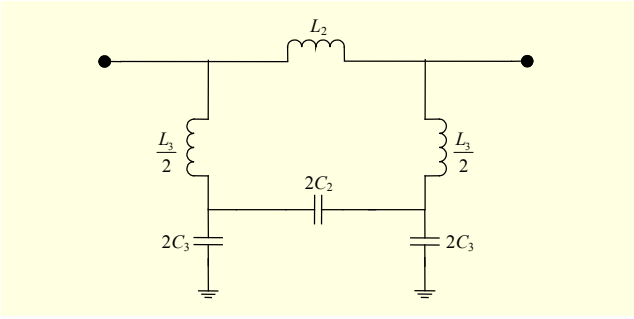

Fig. 3. Simplified LC equivalent circuit of proposed U-shaped resonator.

smaller values of C_2, the two shunt-connected series LC resonators (L_3, C_3) will be isolated having no connection to each other; therefore, the resonance frequency of the two resonators will be equal to around 6 GHz, which results in a deep transmission zero with around 140 dB attenuation. By contrast, for larger values of C_2, the two resonators are correlated and introduce two different zeroes with around 70 dB attenuation, as shown in Fig. 2(b). Thus, to alter the position of the center of multiple zeroes, L_3 and C_3 must be modified, and to alter the distance of the two separate zeroes from their center, C_2 should be modified. So, two completely adjustable transmission zeroes are realized.

To demonstrate the dominant effects of C_2, C_3, and L_3 on the locations of transmission nulls, the extracted LC circuit will be analyzed in detail as follows. By exploiting the symmetry of the LC equivalent circuit shown in Fig. 1(b) and owing to the fact that C_1 and L_1 do not have any effect on the locations of transmission zeroes, the LC circuit in Fig. 1(b) is redrawn in Fig. 3. Based on the concept of a transmission zero, in which there is no signal at the output of the circuit, a fourth-order polynomial equation is yielded (see (1)). The roots of (1) are the transmission zeroes of the proposed novel U-shaped resonator. Since L_2 does not appear in α and the value of the second term in β, $2L_2C_2$, is considerably smaller than the first term, $2L_3(C_2 + C_3)$, it can be concluded that L_2 has an insignificant effect on the location of transmission zeroes. In other words, C_2, C_3, and L_3 control the location of transmission zeroes.

$$(S^2\sqrt{\alpha}+1)^2 + S^2(-2\sqrt{\alpha}+\beta) = 0\,, \qquad (1)$$

$$\alpha = L_3^2\, C_3\left(2C_2 + C_3\right),\quad \beta = 2L_3\left(C_2 + C_3\right) + 2L_2C_2\,,$$

$$\mathrm{f}_1, \mathrm{f}_{2(\mathrm{GHz})} = \frac{25}{\pi} \times \frac{\sqrt{0.1(2\sqrt{\alpha}+\beta)} \pm \sqrt{0.1(-2\sqrt{\alpha}+\beta)}}{\sqrt{\alpha}}$$

One of the features of the proposed U-shaped resonator is that the introduced transmission zeroes can be modified for different applications. Accordingly, the widths of w_2 and w_5

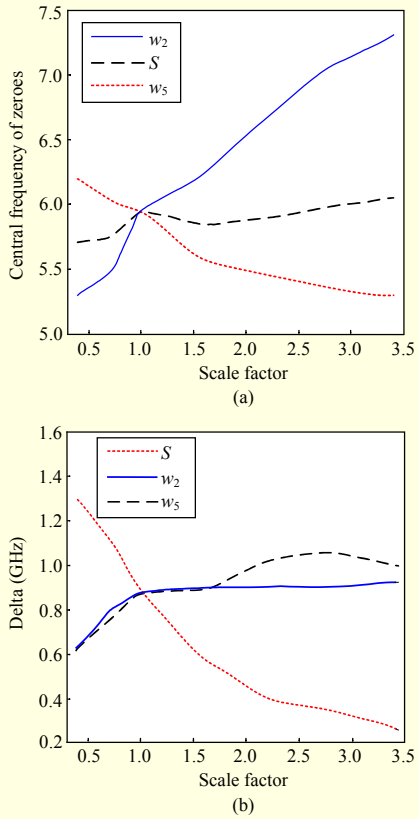

Fig. 4. Adjustability of U-shaped resonator: (a) tuning center frequency and (b) tuning distance between two separate zeroes (delta).

determine the location of the center frequency of the multiple zeroes, while the separation of S determines the distance of the multiple zeroes from the center frequency, by increasing w_2 and decreasing w_5, both the inductance of L_3 and the capacitance of C_3 decrease. This causes the center frequency of the multiple zeroes to shift to a higher frequency, as shown in Fig 4(a). In this case, the effect of variation of S on the center frequency is negligible in comparison with the effects of w_5 and w_2. On the other hand, a decrease in S results in an increase in the value of the coupling capacitor (C_2), which causes the near and far band transmission zeroes to shift to lower and higher frequencies, respectively, as shown in Fig. 4(b). In this case, the effects of altering w_5 and w_2 are insignificant.

III. LPF Design

To sharpen the frequency response of the proposed fully adjustable suppressing cell, a T-shaped resonator is connected to the main high impedance line, which acts as a shunt connected series L-C resonator (as named L_4 and C_4 in Fig. 5(b)). This resonator introduces a transmission zero at around 2.7 GHz, which can be easily calculated by (2). C_4 and

L_4 can be obtained from (3) and (4) as 4.29 nH and 0.63 pF, respectively. In these equations, Z_{OC}, λ_{gC} and Z_{OL}, λ_{gL} correspond to low- and high-impedance lines, respectively. It should be noted that due to some disregarded discontinuity effects, there is an insignificant 10% discrepancy between the calculated resonance frequency by (4) and the obtained value by the EM simulation in Fig. 5(d).

$$f_r = \frac{1}{2\pi\sqrt{C_4 L_4}}, \tag{2}$$

$$L_4 = \frac{1}{\omega_c} Z_{OL} \sin\left(\frac{2\pi}{\lambda_{gL}} l_L\right) + \frac{1}{\omega_c} Z_{OC} \tan\left(\frac{\pi}{\lambda_{gC}} l_C\right), \tag{3}$$

$$C_4 = \frac{l_C}{Z_{OC} v_p} + \frac{1}{\omega_c} \frac{1}{Z_{OL}} \tan\left(\frac{\pi l_L}{\lambda_{gL}}\right), \tag{4}$$

where $v_p = \frac{c}{\sqrt[2]{\varepsilon \text{eff}}}$.

The presence of this T-shaped resonator not only causes the coupling capacitor (C_2) to turn into two coupling capacitors (C_2'), but it also divides L_2 into two equal inductors ($L_2/2$) as shown in Fig. 5(b). Finally, since the inductance line in the T-shaped resonator is really thin, the final equivalent circuit is yielded in Fig. 5(c). As it can be seen from Fig. 5(c), this circuit has maintained the same topology as that of the LC circuit in Fig. 1(b). Indeed, adding the T-shaped resonator makes the coupling distance narrower, and as a result, the value of the coupling capacitor increases from $C_2 = 0.003$ in Fig. 1(b) to $C_2 = 0.0042$ in Fig. 5(c). Thus, by increasing the distance between the edge of the U-shaped resonator and the vertical part of the T-shaped resonator (S'), the coupling distance is extended. Consequently, this leads to a reduction in the value of C_2, resulting in a smaller delta (which means a closer distance between transmission zeros). So, the roles of the coupling distance (S and S') and C_2 have remained unchanged after connecting the T-shaped resonator. All values pertaining to the lumped elements are tabulated in Table 1.

To expand the stopband to 26 GHz, four open radial stubs are used. Figure 6 shows the layout and insertion loss of the proposed radial stubs. The dimensions of the four stubs are calculated to create four transmission zeros to suppress four transmission poles located at 9.35 GHz, 12.37 GHz, 17.4 GHz, and 19.27 GHz. The dimensions for the first to forth stub are $w = 0.2$ mm, 2.3 mm, 4.2 mm, and 3.1 mm, respectively. It is also possible to modify the proposed filter to suit different applications, since the cut-off frequency is controlled mostly by l_6, w_6, and w_7. As is shown in Fig. 7, by increasing both l_6 and w_6 and decreasing w_7, the near-band transmission zero moves to a lower frequency and the passband becomes narrower. This is because by increasing both l_6 and w_6, the capacitance of C_4 increases; and by decreasing w_7 the inductance of L_4 increases. These changes result in a smaller cut-off frequency.

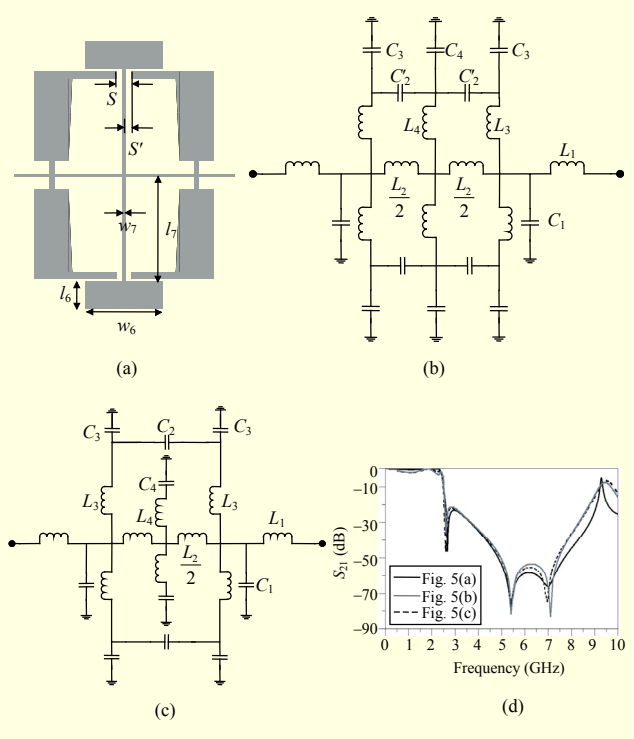

Fig. 5. (a) U-shaped resonator after adding T-shaped resonator ($l_6 = 1.6$ mm, $l_7 = 6.37$ mm, $w_6 = 4.5$ mm, $w_7 = 0.13$ mm); (b) and (c) equivalent circuits of Fig. 5(a); and (d) EM and circuit simulation results.

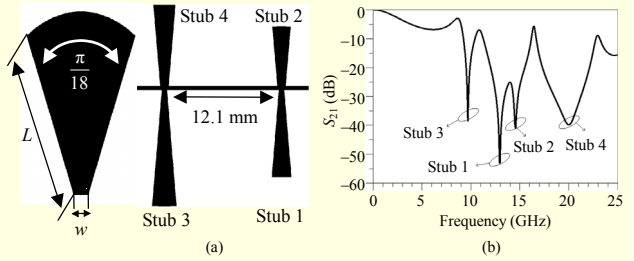

Fig. 6. (a) Proposed radial stubs and (b) frequency response of four radial stubs.

Table 1. Values of lumped elements (units: C, pF; L, nH).

Fig.	C_1	C_2	C_3	C_4	C_2'	L_1	L_2	L_3	L_4
1(b)	1.22	0.0030	1.20			0.61	3.5	0.60	
5(b)	1.72		1.01	0.64	0.057	0.61	3.5	0.66	4.50
5(c)	1.72	0.0042	1.01	0.72		0.61	3.5	0.66	5.24

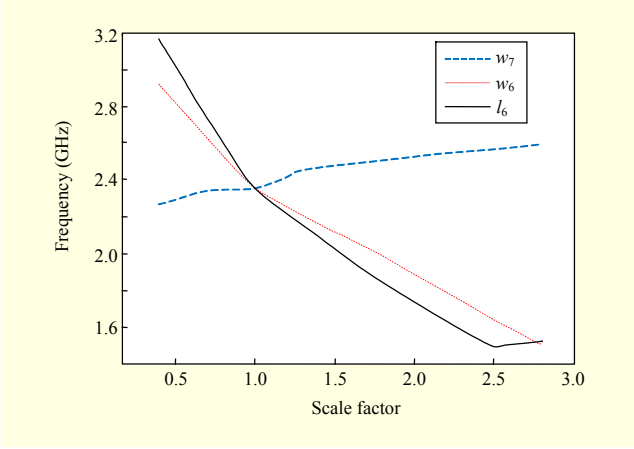

Fig. 7. Cut-off frequency as function of scaling factor.

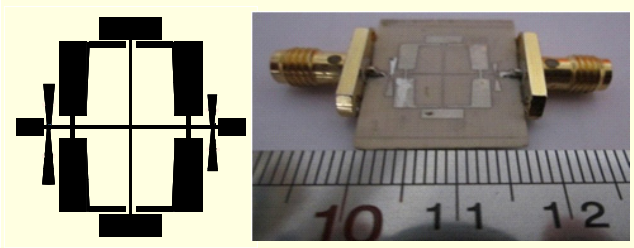

(a) (b)

Fig. 8. (a) Layout of proposed filter and (b) photograph of fabricated filter.

IV. Simulation and Experimental Results

The proposed LPF has been implemented on a substrate with a relative dielectric constant $\varepsilon_r = 3.38$, thickness $h = 0.508$ mm, and loss tangent $\tan\delta = 0.002$. Simulations are done by an EM-simulator (ADS Momentum). The S-parameter is measured by an Agilent network analyzer N5230 A. Figure 8 shows a final layout and a photograph of the fabricated prototype. It can be seen from Fig. 9 that the filter has a 3 dB cut-off frequency equal to 2.35 GHz, an insertion loss of less than 0.6 dB in the passband from DC to 2 GHz, a return loss better than 10.6 dB, and a suppression level higher than 22 dB from 2.53 GHz up to 26 GHz. Thus, the proposed filter has the property of 11 harmonic suppression. Although some spurs exist in the stopband due to the inherent presence of harmonics in the microstrip line, all spurs have been kept below –22 dB by a proper design. The relative stopband bandwidth of the LPF is about 164%. Furthermore, the size of the proposed filter is only 12.9×16.1 mm^2, which corresponds to $0.16\lambda_g \times 0.20\lambda_g$. The return loss in the stopband region is very small, indicating negligibly small radiation loss. The transition band from 2.35 GHz to 2.53 GHz with –3 dB and –20 dB, respectively, is 0.18 GHz, showing that the filter has excellent skirt performance.

Table 2. Performance comparisons among previous filters and proposed one.

Ref.	RO (ζ)	RSB	SF	NCS	AF	FOM
[2]	30	1.25	1.5	0.08×0.08	1	8,789
[3]	95	1.40	2.0	0.21×0.10	1	11,951
[4]	36	1.32	1.5	0.07×0.07	1	11,534
[5]	37	1.65	1.5	0.11×0.09	1	9,065
[6]	22	1.55	1.5	0.09×0.08	1	7,095
[8]	200	1.41	2.0	0.60×0.30	1	2,805
[9]	46	1.37	2.0	0.25×0.15	1	3,279
[10]	74	1.70	1.7	0.13×0.31	1	5,306
[11]	82	1.28	2.5	0.11×0.22	1	10,842
[12]	62	1.72	3.0	0.310×0.24	1	4,430
This work	135	1.64	2.2	0.16×0.20	1	15,221

Note: RO means roll-off rate according to 3 dB and 40 dB attenuation points, RSB means relative stopband bandwidth, SF means suppression factor, NCS means normalized circuit size, and AF means the architecture factor.

$$\text{FOM} = \frac{\zeta \times \text{RSB} \times \text{SF}}{\text{NCS} \times \text{AF}}$$

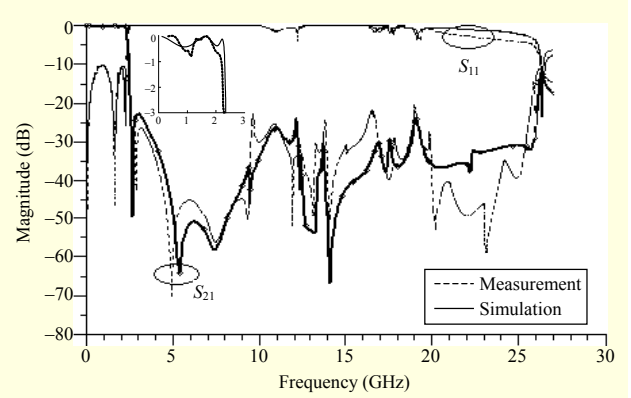

Fig. 9. Simulated and measured S-parameters of proposed low-pass filter.

For comparison, Table 2 compares the performance of the proposed filter with that of some of the latest filters based on several specifications explained in [4]. According to Table 2, the presented filter exhibits a high figure-of-merit (15,221) among the quoted filters.

V. Conclusion

A compact LPF with sharp roll-off and wide stopband bandwidth is proposed and implemented. The filter is composed of a U-shaped fully adjustable resonator, four radial stubs, and a T-shaped resonator. The first two sections contribute to the creation of an ultra-wide stopband, while the T-shaped resonator provides a fully adjustable cut-off

frequency with a very sharp roll-off. The results indicate that the demonstrated filter achieves very high figure-of-merit in comparison to the latest fabricated filters. With the above desirable features, the proposed filter could be employed for microwave communication applications.

References

[1] J.S. Hong and M.J. Lancaster, "*Microstrip Filters for RF/Microwave Applications*," New York, NY, USA: John Wiley & Sons, Inc., 2001, pp. 109–158.

[2] X.B. Wei et al., "Compact Wide-Stopband Low-Pass Filter Using Stepped Impedance Hairpin Resonator with Radial Stubs," *IET Electron. Lett.*, vol. 47, no. 15, July 2011, pp. 862–863.

[3] V.K. Velidi and S. Sanyal, "Sharp Roll-off Low-Pass Filter with Wide Stopband Using Stub-Loaded Coupled-Line Hairpin Unit," *IEEE Microw. Wireless Compon. Lett.*, vol. 21, no. 6, June 2011, pp. 301–303.

[4] J. Wang et al., "Compact Quasi-Elliptic Microstrip-Low-Pass Filter with Wide Stopband," *IET Electron. Lett.*, vol. 46, no. 20, Sept. 2010, pp. 1384–1385.

[5] J. Wang, H. Cui, and G. Zhang, "Design of Compact Microstrip-Low-Pass Filter with Ultra-wide Stopband," *IET Electron. Lett.*, vol. 48, no. 14, July 2012, pp. 854–856.

[6] J. Xu et al., "Design of Miniaturized Microstrip LPF and Wideband BPF with Ultra-wide Stopband," *IEEE Microw. Wireless Compon. Lett.*, vol. 23, no. 8, Aug. 2013, pp. 397–399.

[7] H. Cui, J. Wang, and G. Zhang, "Design of Microstrip Low-Pass Filter with Compact Size and Ultra-wide Stopband," *IET Electron. Lett.*, vol. 48, no. 14, July 2012, pp. 856–857.

[8] R. Gómez-García et al., "Extended-Stopband Microstrip Low-Pass Filter Using Rat-Race Directional Couplers," *IET Electron. Lett.*, vol. 49, no. 4, Feb. 2013, pp. 272–274.

[9] H. Sariri et al., "Compact LPF Using T-Shaped Resonator," *Frequenz J.*, vol. 67, no. 1–2, Jan. 2013, pp. 17–20.

[10] A. Abbosh, "Low-Pass Filter Utilizing Broadside-Coupled Structure for Ultra-wide Band Harmonic Suppression," *IET Microw. Antennas Propag.*, vol. 6, no. 3, Feb. 2012, pp. 276–281.

[11] C.-J. Wang and C.-H. Lin, "Compact Low-Pass Filter with Sharp Transition Knee by Utilizing a Quasi-Slot Resonator and Open Stubs," *IET Microw. Antennas Propag.*, vol. 4, no. 4, Apr. 2010, pp. 512–517.

[12] K. Ma and K.S. Yeo, "New Ultra-wide Stopband – Low-Pass Filter Using Transformed Radial Stubs," *IEEE Trans. Microw. Theory Techn.*, vol. 59, no. 3, Mar. 2011, pp. 604–611.

[13] G. Karimi, A. Lalbakhsh, and H. Siahkamari, "Design of Sharp Roll-off Low-Pass Filter with Ultra-wide Stopband," *IEEE Microw. Wireless Compon. Lett.*, vol. 23, no. 6, June 2013, pp. 303–305.

[14] A.A. Lotfi-Neyestanak and A. Lalbakhsh, "Improved Microstrip Hairpin-Line Bandpass Filters for Spurious Response Suppression," *IET Electron. Lett.*, vol. 48, no. 14, July 2012, pp. 858–859.

[15] M. Hayati et al., "A Novel Miniaturized Wilkinson Power Divider with *N*th Harmonic Suppression," *J. Electromagn. Waves Appl.*, vol. 27, no. 6, Apr. 2013, pp. 726–735.

Gholamreza Karimi received his BS, MS, and PhD degrees in electrical engineering from Iran University of Science and Technology, Tehran, Iran, in 1999, 2001, and 2006, respectively. Since 2007, he has been with the Electrical Department, Razi University, Kermanshah, Iran, where he is now an associate professor. His main research interests are low power analog and digital IC design; RF IC design; and modeling and simulation of RF/mixed signal IC. He is also interested in microwave devices and artificial intelligence systems.

Ali Lalbakhsh received his BS degree in communication engineering from Islamic Azad University, Boroujerd, Iran, in 2008 and his MS degree in communication engineering from Islamic Azad University, Science and Research Branch, Tehran, Iran, in 2011. From 2010, he has been lecturing at Islamic Azad University, Kermanshah, Iran. His research interests are microwave passive and active components; antenna design; periodic and electromagnetic band gap structures; and evolutionary algorithms. He has been a member of both the Institute of Electrical and Electronics Engineers and the Institute of Electronics, Information and Communication Engineers since 2011. He has also served as a reviewer for several journals.

Khatereh Dehghani received her BS degree in electrical engineering from Islamic Azad University, Science and Research Branch, Tehran, Iran, in 1996 and her MS degree in electrical engineering, from Islamic Azad University, Science and Research Branch, Kermanshah, Iran, in 2013. Her research interest is RF/microwave circuit design.

Hesam Siahkamari received his BS degree in electrical engineering from Islamic Azad University, Kermanshah, Iran, in 2010 and his MS degree in electrical engineering from Razi University, Kermanshah, Iran, in 2013. His current research interest is RF/microwave circuit design.